

Optimization of ANFIS Network Using Particle Swarm Optimization Modeling of Scour around Submerged Pipes

Rahim Gerami Moghadam¹ · Saeid Shabanlou¹ · Fariborz Yosefvand¹

Received: 6 November 2019 / Accepted: 6 June 2020 / Published online: 8 October 2020
© Harbin Engineering University and Springer-Verlag GmbH Germany, part of Springer Nature 2020

Abstract

In general, submerged pipes passing over the sedimentary bed of seas are installed for transmitting oil and gas to coastal regions. The stability of submerged pipes can be threatened with waves and coastal flows occurring at coastal regions. In this study, for the first time, the adaptive neuro-fuzzy inference system (ANFIS) is optimized using the particle swarm optimization (PSO) algorithm, and a meta-heuristic artificial intelligence model is developed for simulating the scour pattern around submerged pipes located in sedimentary beds. Afterward, six ANFIS-PSO models are developed by means of parameters affecting the scour depth. Then, the superior model is detected through sensitivity analysis. This model has the function of all input parameters. The calculated correlation coefficient and scatter index for this model are 0.993 and 0.047, respectively. The ratio of the pipe distance from the sedimentary bed to the submerged pipe diameter is introduced as the most effective input parameter. PSO significantly improves the performance of the ANFIS model. Approximately 36% of the scour depths simulated using the ANFIS model have an error less than 5%, whereas the value for ANFIS-PSO is roughly 72%.

Keywords Adaptive neuro-fuzzy inference system (ANFIS) · Meta-heuristic model · Particle swarm optimization (PSO) · Scour around submerged pipes · Coastal regions

1 Introduction

Nowadays, given the operation of undersea oil and gas reservoirs located in coastal regions, the transport of these fossil fuels to lands requires the use of pipelines. Pipelines are generally placed near erodible sea beds, and scour formation can possibly occur due to the existence of flows and waves. As an

erodible bed is scoured, the stability of pipelines is threatened with the risk of large deformations and failure.

Thus, given the importance of this issue, experimental, analytical, and numerical studies have been carried out on the scour pattern in the vicinity of submerged pipelines. Fredsoe et al. (1988) experimentally investigated the two-dimensional scour pattern in the vicinity of submerged pipes located horizontally on a sedimentary bed. Through the analysis of experimental results, they forecasted the development pattern of the scour hole as horizontal. Sumer and Fredsoe (1990) proposed an equation to estimate the scour around submerged pipes. They evaluated the influence of waves created from the interaction between the sedimentary bed and pipelines. Chiew (1993) conducted experimental measurements on the behavior of sheets installed on pipelines and showed that the existence of these sheets intensified the scouring process in the vicinity of submerged pipes. Brørs (1999) simulated the scour pattern around submerged pipes placed horizontally on a sedimentary bed by developing a numerical model. He implemented Navier–Stokes equations for solving the flow field. He compared the results of his model with the experimental data and stated that the model had reasonable accuracy. Moncada-M and Aguirre-Pe (1999)

Article Highlights

- The adaptive neuro-fuzzy inference system (ANFIS) was optimized using the particle swarm optimization (PSO), and ANFIS-PSO model was defined.
- The scour depth around submerged pipes located in sedimentary bed was estimated using the ANFIS-PSO model.
- The most important parameters affecting the scour depth were identified.
- The performance of ANFIS-PSO model was compared with the ANFIS network, with a superiority of ANFIS-PSO.

✉ Saeid Shabanlou
saeid.shabanlou@gmail.com

¹ Department of Water Engineering, Kermanshah Branch, Islamic Azad University, Kermanshah 6718997551, Iran

conducted an experimental study and showed that the Reynolds number had no significant effect on the scour pattern around horizontal submerged pipes. Furthermore, they stated that by increasing the Froude number, the dimensions of the scour hole increased. Sumer et al. (2001) carried out an experimental research and evaluated the scour process around submerged pipes subjected to waves and flows. They observed that by starting the scour process, the scour hole expanded longitudinally along the pipeline. Myrhaug and Rue (2003) provided separate relationships for estimating the scour pattern in terms of the depth and width of the scour hole in regular and random wave conditions. They compared the results of their analytical study with the experimental values. Teh et al. (2006) examined the stability of horizontal submerged pipes located on loose soils by conducting an analytical study and investigated the fracture mechanism of pipes. Furthermore, they measured the pipe penetration into soil. Dey and Singh (2008) experimentally studied the scour depth in the vicinity of submerged pipes in clear-water condition. They studied the effect of various hydraulic and geometric parameters on the scour pattern and stated that the scour hole dimensions increased with the increase in the depth of inflow. Wu and Chiew (2012) conducted an experimental research on the scour behavior around submerged pipes located on sedimentary beds and exhibited that the Froude number and Shields parameter are the most effective factors of scour pattern. Additionally, Azamathulla et al. (2014) studied scour pattern in the vicinity of the submerged skewed pipeline in an open channel experimentally.

The neural network and artificial intelligence (AI) models have been widely used in modeling nonlinear systems and solving complex problems in various sciences. These modeling techniques are also used in different fields (Najafzadeh et al. 2014a; Azimi et al. 2017; Bonakdari and Ebtehaj 2017; Shabanlou et al. 2018; Azimi et al. 2019a). Azamathulla and Ab Ghani (2012) modeled the scour pattern around submerged pipes in the vicinity of the live bed using the gene programming (GP) model. They compared the results of their model with those of an artificial neural network and concluded that the GP model has higher accuracy. Furthermore, Etemad-Shahidi et al. (2011) proposed relationships for predicting the scour amount around horizontal pipes located on the sedimentary bed in the clear condition using the M5' learning machine. Najafzadeh et al. (2014a) predicted the scour pattern around submerged pipes located on the sedimentary bed. They used the group method of data handling (GMDH), the adaptive neuro-fuzzy inference system (ANFIS) model, the tree model, and empirical relationships and, by evaluating the results of these models, indicated that GMDH had the highest accuracy. Najafzadeh et al. (2014b) simulated the scour pattern around the pipes in clear-water and live-bed circumstances by means of GMDH. Azimi et al. (2019b) developed a hybrid AI model to predict the scour around

abutments. The authors combined the genetic algorithm and singular-value decomposition with ANFIS network to enhance the performance of simulation. Furthermore, Azimi and Shiri (2020) evaluated the scour around subsea pipelines by using gene expression programming (GEP). They performed a sensitivity analysis to introduce the best GEP model and the most important and effective parameters.

On the one hand, the vast majority of crude oil and natural gases exploited in coastal regions are transported to land by means of submerged pipelines. Additionally, the stability of pipelines can be endangered because of scouring and erosion around the infrastructures built at coastal districts. Thus, the estimation and modeling of scour around submerged pipelines play a crucial role in providing a safe and cost-effective design.

On the other hand, AI techniques have been broadly used in simulating numerous problems, accompanied by increasing number of related studies. The AI methods are cheap, fast, and accurate in predicting different phenomena.

Therefore, in the present study, for the first time, a novel hybrid AI technique is employed to simulate the scour around submerged pipelines. The ANFIS model and particle swarm optimization (PSO) algorithm are combined, and a meta-heuristic model named "ANFIS-PSO" is developed to estimate the scour depth for the first time. All input parameters affecting the scour depth around submerged pipelines are introduced, and six ANFIS-PSO models are defined using the input parameters. Through sensitivity analysis, the superior ANFIS-PSO model and the most effective input parameter are detected. Finally, the ANFIS and ANFIS-PSO models are compared.

2 Materials and Methods

2.1 Experimental Model

The experimental values measured by Moncada-M and Aguirre-Pe (1999) are used to verify the results of the numerical models. The experimental model is composed of a rectangular flume with a length of 8.3 m, a width of 0.5 m, and a height of 0.5 m. The submerged pipes in four different sizes are placed horizontally on an erodible bed. Two types of sediments are used for the experiments. Table 1 lists the range of experimental values used in this study. Figure 1 illustrates the schematic layout of the experimental model and scour pattern around the submerged pipes.

2.2 Adaptive Neuro-Fuzzy Inference System

Jang (1993) provided the ANFIS that can combine the two mentioned methods. This method is practically developed in the field of engineering. ANFIS has a good ability to learn,

Table 1 Experimental measurements used in this study

Parameter	e/D	D/d_{50}	y/D	τ^*	Fr	d_s/D
Range	0–1.068	3.289–66.667	1.067–5	0.038–0.665	0.234–0.836	0.008–1.0606

construct, and classify. It also allows the extraction of fuzzy rules from numerical information of expert knowledge and adaptively establishes a rule. Furthermore, ANFIS can adjust the complex transformation of mankind intelligence into fuzzy systems. The main problem is that the ANFIS prediction model requires considerable time to learn the structure and determine parameters. For simplification, we assume that the interference system requires two inputs (x and y) and an output (y). Figure 2 provides the architecture of an ANFIS network (Jang 1993).

For a first-order Takagi–Sugeno fuzzy model, a sample rule set with two fuzzy if-then rules can be expressed as follows (Jang 1993):

Rule 1: If x is A_1 , and y is B_1 , then:

$$z_1 = p_1x + q_2y + r_1 \tag{1}$$

Rule 2: If x is A_2 , and y is B_2 , then:

$$z_2 = p_2x + q_2y + r_2 \tag{2}$$

where $\{r_1p_1, q_1, r_2, p_2, q_2\}$ are the linear parameters in the antecedent part of the first-order Takagi–Sugeno fuzzy model. The structure of the ANFIS system includes five layers (Jang 1993).

First layer (input nodes): Each node of this layer produces membership values belonging to appropriate fuzzy sets using the membership function.

Second layer: The AND operator is utilized to obtain the output (firing strength) representing the front part of that rule. Firing strength is the front part of an estimated fuzzy rule which forms the output function of that rule.

Third layer (medium nodes): The main objective in the third layer is to determine the ratio of each firing strength as the i th rule to the sum of all firing strength of rules.

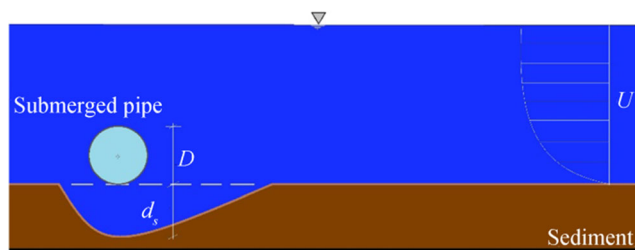


Figure 1 Schematic layout of experimental model and scour pattern around submerged pipes

Fourth layer (result nodes): The node function of the fourth layer calculates the distribution layer of the i th rule to the total output.

Fifth layer (output node): This single node calculates the total output by summing all input signals. Thus, in this layer, the nonfuzzy making process alters the results of each fuzzy rule to a nonfuzz output.

Modeling of the ANFIS system requires the definition of the provided method to produce the fuzzy interference system. In this study, the fuzzy clustering method is used. In fuzzy systems, the accuracy and validity of the trained ANFIS system depend on structural parameters and parameters related to learning of these systems. Parameters related to learning include the optimization method, the rate of increase and decrease in steps, and the termination criterion of the learning process. Furthermore, the trained system must comprise correct answers in the new error condition. The size and shape of these systems are important factors, because by increasing the number of membership functions, the if-then fuzzy rules in the network structure grows larges. As a result, the generalization characteristics of ANFIS for predicting the data decrease. The membership function includes various adjustable parameters that must be optimized for reaching the optimized modeling. Thus, a stronger algorithm is needed for defining values. Several optimization algorithms can enhance the performance of fuzzy systems. The PSO algorithm is one of such algorithms that are suitable for optimization. This algorithm can minimize the error between the model output and the real value of learning data (Jang 1993).

2.3 Particle Swarm Optimization Algorithm (PSO)

PSO is a group intelligence method developed by Eberhart and Kennedy (1995). This algorithm is inspired by the social behavior of birds in constructing nests. PSO is a population-based method in which each particle represents a solution. The

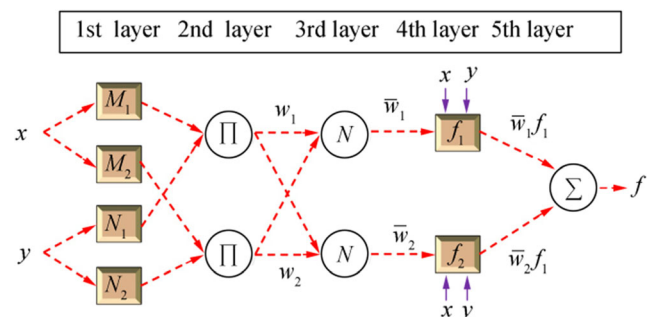


Figure 2 Architecture of ANFIS network

situation of particles in the search environment is determined by two factors: situation and speed. Given that each population includes m particles in the M -dimension problem environment, the situation (x) and speed (v) of particle i are respectively defined as follows (Eberhart and Kennedy 1995):

$$x_i = (x_{i1}, x_{i2}, \dots, x_{iD}) \quad i = 1, 2, \dots, m \tag{3}$$

$$v_i = (v_{i1}, v_{i2}, \dots, v_{iD}) \tag{4}$$

The optimization process of PSO starts with a randomly selected population, which is then optimized for updating generations, in the search environment. Each particle is updated based on two distinctive particles. The first particle ($p_{best} = (p_{i1}^t, p_{i2}^t, \dots, p_{iD}^t)$) is the best solution achieved by the particles thus far. The second particle $g_{best} = (p_{g1}^t, p_{g2}^t, \dots, p_{gD}^t)$ is the best result achieved by all particles in the population. The fundamental relationships of the PSO algorithm can be provided as follows (Eberhart and Kennedy 1995):

$$v_{id}^{t+1} = w \cdot v_{id}^t + c_1 \times \text{rand}_1 \times (p_{id}^t - x_{id}^t) + c_2 \times \text{rand}_2 \times (p_{gd}^t - x_{id}^t) \tag{5}$$

$$x_{id}^{t+1} = x_{id}^t + v_{id}^{t+1} \tag{6}$$

where v_{id}^{t+1} is the velocity of the i th particle in t iteration, c_1 and c_2 are positive constant values, and w_i is the inertia weight controlling the influence of previous velocity of particles on current velocities. Two random variables are distributed in the range of 0 to 1. x_{id}^{t+1} is the current situation of the i th particle. A restricting factor is introduced to the PSO standard algorithm to ensure the search convergence; then, the following equation is provided (Eberhart and Kennedy 1995):

$$v_{id}^{t+1} = \chi [v_{id}^t + c_1 \times \text{rand}_1 \times (p_{id}^t - x_{id}^t) + c_2 \times \text{rand}_2 \times (p_{gd}^t - x_{id}^t)] \tag{7}$$

$$\chi = \frac{2}{|2 - \varphi - \sqrt{\varphi^2 - 4\varphi}|} \tag{8}$$

According to the above equation, χ is restricted by c_1 and c_2 . The vibration range of particles decreases when they reach the best position. However, despite the (ANFIS) $V_{max} = X_{max}$ limitation, the particles can achieve a desirable performance. Evidently, a restricting factor in PSO provides a better solution than the standard PSO.

2.4 Parameters Affecting the Scour Around Submerged Pipes

Moncada-M and Aguirre-Pe (1999) stated that the scour in the vicinity of horizontal submerged pipes (d_s) is a function of parameters, such as the flow average velocity (U), normal

flow depth (y), density of water (ρ), density of sediments (ρ_s), dynamic viscosity of water (μ), channel slope (S_0), channel width (B), diameter of bed materials (d_{50}), pipe diameter (D), distance between the pipe and sedimentary bed before scour (e), and acceleration of gravity (g). The following is then obtained:

$$d_s = f(U, y, \rho, \rho_s, \mu, S_0, B, d_{50}, D, e, g) \tag{9}$$

In addition, Moncada-M and Aguirre-Pe (1999) introduced eight dimensionless groups using the Buckingham theory and rewrote Eq. (15) as follows:

$$\frac{d_s}{D} = f\left(Fr, Re, \tau^*, \frac{y}{D}, \frac{D}{d_{50}}, \frac{e}{D}, S_0, \frac{y}{B}\right) \tag{10}$$

In Eq. (15), $Fr = U/\sqrt{g \cdot y}$, $Re = UD\mu/g$, and $\tau^* = u_*^2/g \cdot (\rho_s/(\rho-1))$. d_{50} are the Froude number, Reynolds number, and Shields parameter, respectively. Moncada-M and Aguirre-Pe (1999) assumed that the channel slope (S_0) is constant, and parameter y/B and the Reynolds number cause no significant influence on the scour pattern, providing Eq. (11) as follows:

$$d_s/D = f(Fr, \tau^*, y/D, D/d_{50}, e/D) \tag{11}$$

In the current numerical study, the effects of the parameters in Eq. (11) are used as the input parameters of various ANFIS-PSO models. Figure 3 shows the combinations of these parameters. In addition, in this study, Monte Carlo simulations are utilized to enhance the

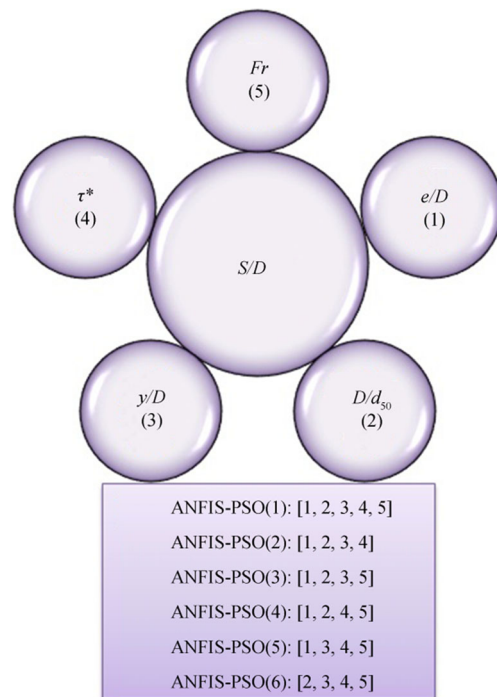


Figure 3 Combinations of input parameters for six ANFIS-PSO models

capability of the ANFIS-PSO models. These simulations are a broad classification of a computational algorithm that uses random sampling for calculating numerical results. The main idea of this approach relies on this basis that using random decision-making attempts to solve problems that might be real in nature. Monte Carlo methods are usually implemented for simulating physical and mathematical systems which are unsolvable when using other methods. Monte Carlo simulation is generally employed using the probability distribution for solving various problems, such as optimization and numerical integration. Furthermore, the k -fold validation method is used in this study for training and testing the mentioned numerical models. In this method, the main sample, which consists of all data, is randomly divided into k subsamples with the same size. Among subsamples, a sample is selected as the testing data, and the remaining data ($k-1$) are used as the training data of numerical models. Then, the k validation procedure is repeated k times, and each subsample is used as the testing data once. In this study, k is considered equal to 6. Figure 4 illustrates the schematic layout of the k -fold cross validation method.

3 Results and Discussion

In this paper, statistical indices, including mean absolute percent error (MAPE), root mean square error (RMSE), scatter index (SI), BIAS index, and the correlation coefficient (R), are used to evaluate the accuracy of the different numerical models (Azimi et al. 2017):

$$MAPE = \frac{1}{n} \sum_{i=1}^n \left(\frac{|(d_s/D)_{(Predicted)_i} - (d_s/D)_{(Observed)_i}|}{(d_s/D)_{(Observed)_i}} \right) \times 100 \quad (12)$$

$$RMSE = \sqrt{\frac{1}{n} \sum_{i=1}^n \left((d_s/D)_{(Predicted)_i} - (d_s/D)_{(Observed)_i} \right)^2} \quad (13)$$

$$SI = \frac{RMSE}{(d_s/D)_{(Observed)}} \quad (14)$$

$$BIAS = \frac{1}{n} \sum_{i=1}^n \left((d_s/D)_{(Predicted)_i} - (d_s/D)_{(Observed)_i} \right) \quad (15)$$

$$R = \frac{\sum_{i=1}^n \left((d_s/D)_{(Observed)_i} - \overline{(d_s/D)_{(Observed)}} \right) \left((d_s/D)_{(Predicted)_i} - \overline{(d_s/D)_{(Predicted)}} \right)}{\sqrt{\sum_{i=1}^n \left((d_s/D)_{(Observed)_i} - \overline{(d_s/D)_{(Observed)}} \right)^2 \sum_{i=1}^n \left((d_s/D)_{(Predicted)_i} - \overline{(d_s/D)_{(Predicted)}} \right)^2}} \quad (16)$$

In these equations, the values of $(d_s/D)_{(Observed)_i}$, $(d_s/D)_{(Predicted)_i}$, and $\overline{(d_s/D)_{(Observed)}}$ are the experimental, predicted, and average experimental scours, respectively, and n is the number of experimental measurements. The closeness of MAPE, RMSE, and SI to zero shows that the AI models have a desirable performance, whereas the closeness of the R index to 1 indicates the highest correlation with observed values.

Subsequently, the accuracy of the developed models is studied. As discussed above, in this study, a hybrid model predicts the scour by combining all input parameters (ANFIS-PSO 1). Then, by eliminating each of the mentioned

parameter, the sensitivity of the model is evaluated in terms of the removed parameter. In other words, the ANFIS-PSO (2) to ANFIS-PSO (6) models predict scour values by combining 4 input parameters. Figure 5 shows the comparison of the observed and predicted scour values by the ANFIS-PSO models. ANFIS-PSO (1) predicts the values of the objective function in terms of all input parameters. Among all mentioned models, this model has the minimum error value and the highest correlation with the experimental values. The calculated values of R and SI for ANFIS-PSO (1) model are 0.993 and 0.047, respectively. The values of $BIAS$ and $RMSE$ for this model are estimated at -1.15×10^{-7} and 0.042, respectively. Furthermore, in the study of the ANFIS-PSO (2) model, the values of R , $RMSE$, and $MAPE$ are equal to 0.973, 0.081, and 15.651, respectively. For this model, the influence of the Froude number is eliminated. In other words, scour values around submerged pipes are modeled in terms of τ^* , y/D , D/d_{50} , and e/D . Among the models with two input parameters, ANFIS-PSO (3) has the highest accuracy. The calculated values of $MAPE$ and $RMSE$ for this model are 12.428 and 0.078, respectively. The calculated values of $R < SI$ and $BIAS$ for the mentioned model are 0.947, 0.089, and -4×10^{-8} , respectively. This function predicts the values of the objective

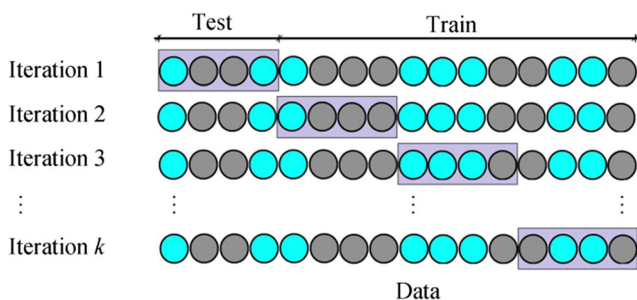


Figure 4 Schematic layout of k -fold cross validation method

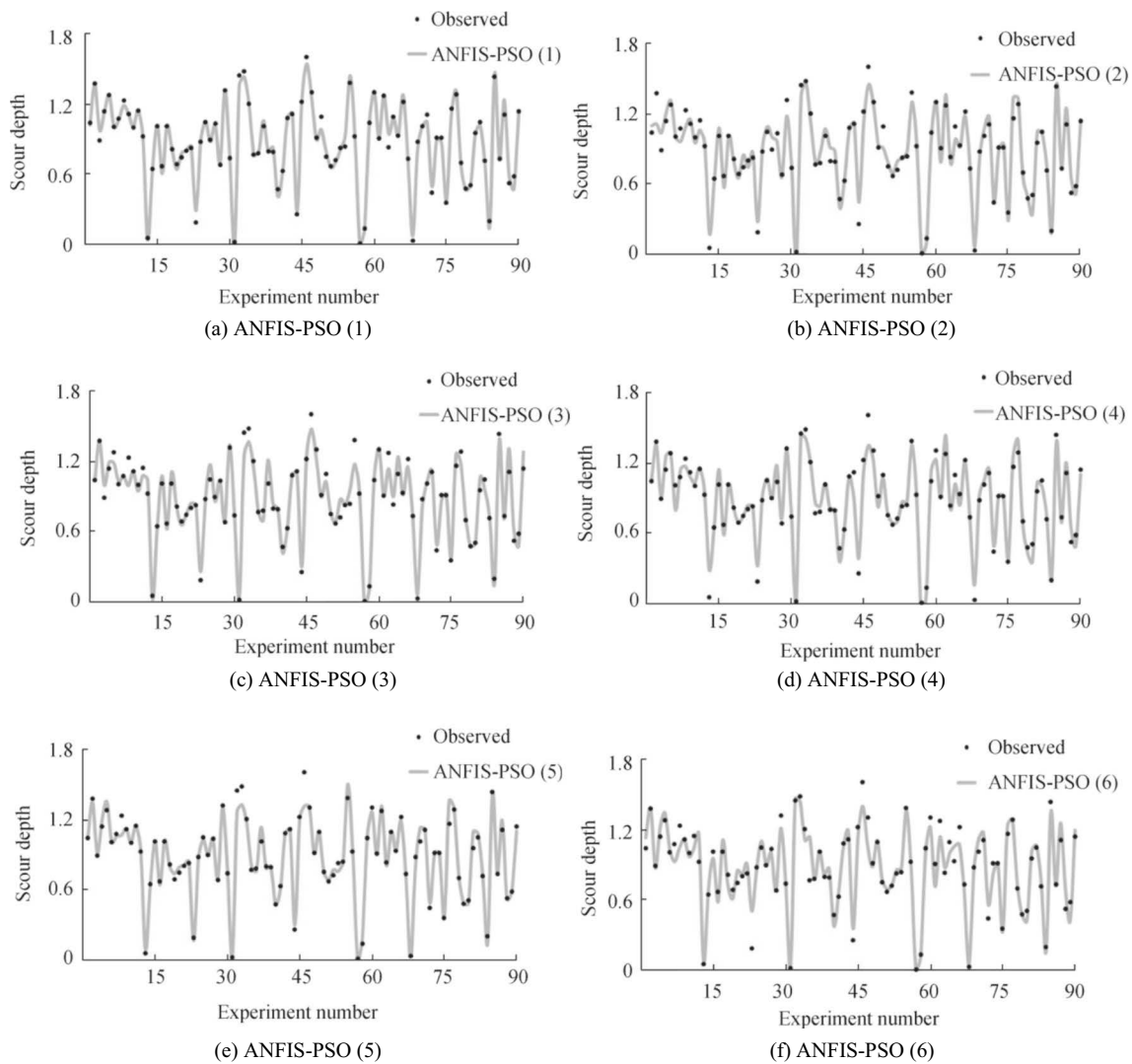


Figure 5 Comparison of observed and predicted values of scour by ANFIS-PSO models

function in terms of Fr , y/D , D/d_{50} , and e/D . For the mentioned hybrid model, the influence of the Shields dimensionless parameter is eliminated due to sediment transport. The study of the ANFIS-PSO (4) model shows the calculated values of SI and R at 0.091 and 0.973, respectively. The values of $BIAS$ and $RMSE$ for this model are -1×10^{-7} and 0.080, respectively. This model predicts the value of d_s/D by eliminating parameter y/D . The ANFIS-PSO (4) model predicts the objective function using Fr , τ^* , D/d_{50} , and e/D . For modeling the scour using the ANFIS-PSO (5) model, the influence of parameter D/d_{50} is neglected. For this model, the values of SI and R approximate are 0.119 and 0.952, respectively. The values of $RMSE$ and $MAPE$ for the mentioned model are 0.105 and 13.647, respectively. Among all the developed hybrid models, ANFIS-PSO (6) has the minimum accuracy. The calculated values of SI , R , and $BIAS$ for this model are 0.154, 0.917, and -1.1×10^{-7} . This model is a function of the dimensionless parameters Fr , τ^* , y/D , and D/d_{50} . In other words,

the influence of e/D in this model is neglected. According to the results of the 6 models, the ANFIS-PSO (1) model has the highest accuracy. Thus, this model is introduced as the superior model. Through the elimination of dimensionless parameter e/D , the modeling accuracy decreases significantly. Thus, this parameter is detected as the most effective parameter.

The discrepancy ratio (DR) is evaluated to further examine the numerical models. This coefficient is defined as follows:

$$(d_s/D)_{(Predicted)_i} - (d_s/D)_{(Observed)_i} \tag{17}$$

The maximum, minimum, and average DR s are denoted by DR_{max} , DR_{min} , and DR_{ave} , respectively. Figure 6 shows the change trend of DR versus the changes in the observed scour. According to Eq. (17), the closeness of the parameter DR represents the closeness of the simulated values to the observed findings. The values of DR_{ave} and DR_{max} for ANFIS-PSO (1)

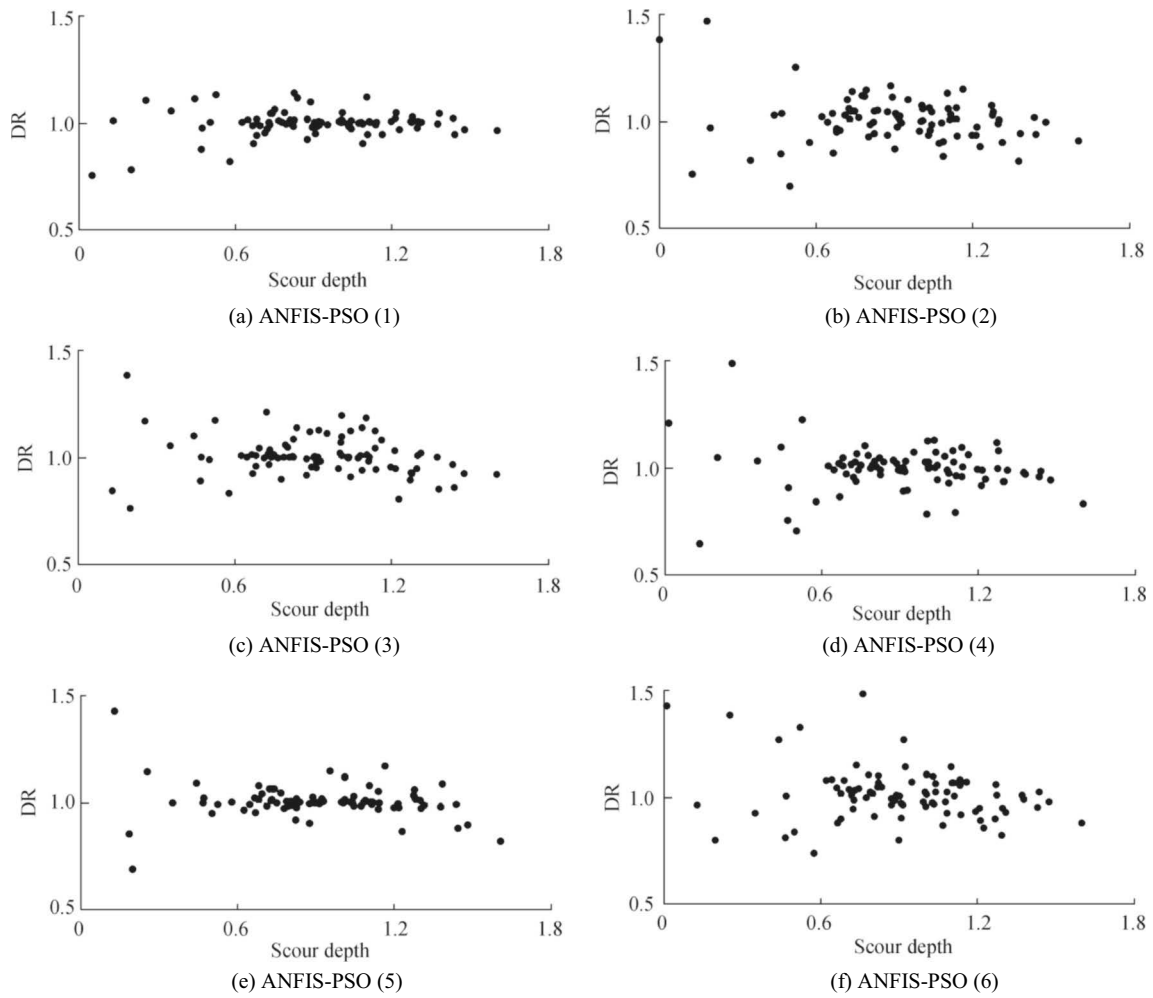


Figure 6 Changes in DR versus observed scour changes

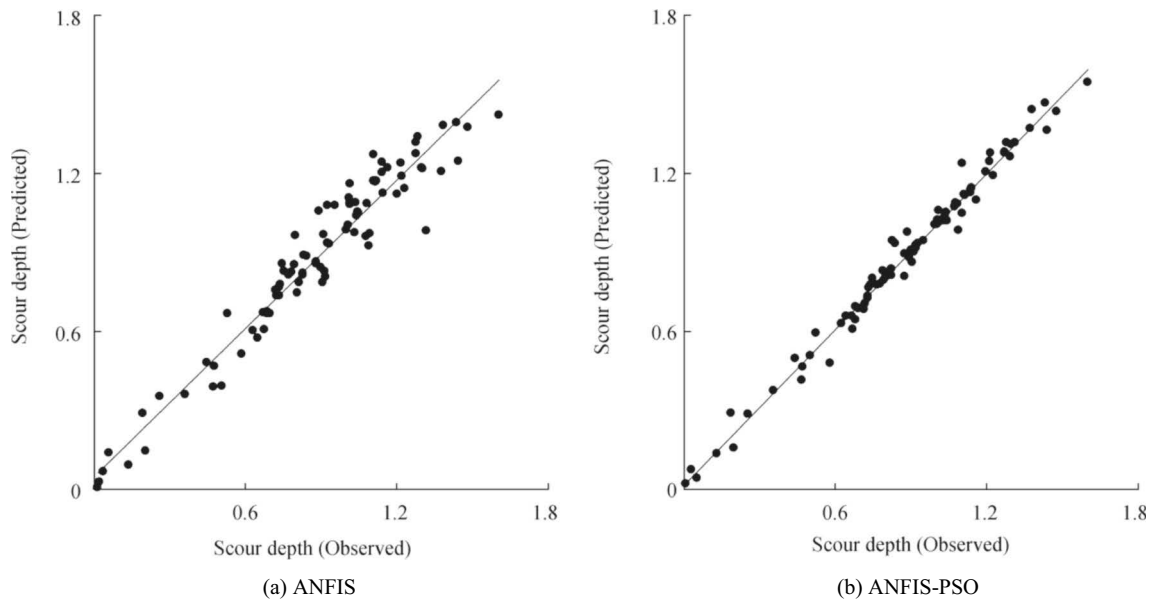


Figure 7 Comparison of scatter plots of ANFIS-PSO with ANFIS

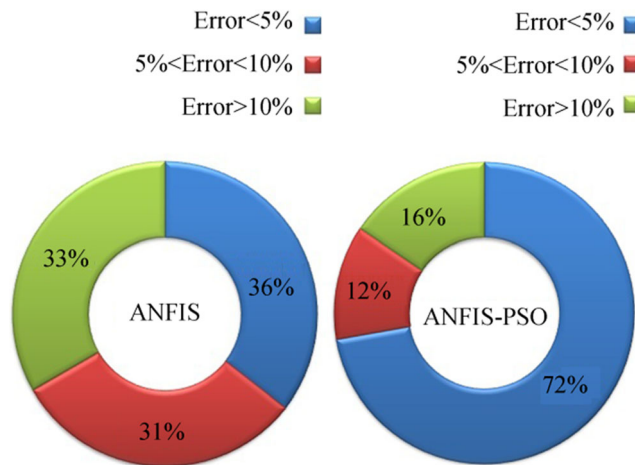


Figure 8 Error distribution for ANFIS and ANFIS-PSO model

reach 1.014 and 2.249, respectively. The values of DR_{ave} for ANFIS-PSO (2) and ANFIS-PSO (3) are 1.011 and 0.996, respectively. The DR_{max} and DR_{ave} for ANFIS-PSO (4) are 5.475 and 1.005, respectively. Furthermore, the DR_{min} for ANFIS-PSO (5) is 0.264. The calculated DR_{max} , DR_{min} , and DR_{ave} for the ANFIS-PSO (5) model are 2.681, 0.730, and 1.048, respectively.

The hybrid superior model (ANFIS-PSO 1) is compared with the ANFIS model. Figure 7 illustrates the scatter plots of the models. The PSO algorithm increases the modeling accuracy significantly. Thus, the mentioned algorithm optimizes the ANFIS model properly. The calculated values of R and SI for the ANFIS model are 0.968 and 0.099, respectively. The values of MAPE and RMSE for this model are 12.441 and 0.087, respectively. Figure 8 depicts the error distribution for ANFIS and ANFIS-PSO. Based on the error distribution, about 36% of the scour depths simulated using the ANFIS model have an error less than 5%, whereas the value for ANFIS-PSO is roughly 72%. Moreover, almost 16% of the results obtained from the ANFIS-PSO model have an error of more than 10%. Therefore, ANFIS-PSO has a better performance in simulating the scour depth around submerged pipelines than ANFIS alone.

4 Conclusions

In this study, by combining the ANFIS model and the PSO algorithm, a meta-heuristic model was developed for simulating the depth of the scour hole around submerged pipes. By detecting the effective factors of scour depth, six distinctive hybrid models were defined. The analysis of the mentioned models indicated the high accuracy of the numerical models. The obtained BIAS and RMSE values for the superior model were -1.5×10^{-7} and 0.042, respectively. The calculated DR_{ave} for the mentioned model was 1.014. This model predicted the scour values in terms of all input parameters and

examination of the input parameters and showed that the ratio of the distance between the pipe and the sedimentary bed to the pipe diameter is the most important and most effective parameter. Subsequently, the hybrid superior model was compared with the ANFIS model. The meta-heuristic model has higher accuracy compared with the ANFIS model. Roughly 36% of the scour depths predicted by using the ANFIS model had an error less than 5%, whereas the value for ANFIS-PSO model was nearly 72%. Additional experimental and numerical studies related to the scour pattern around subsea pipelines should be performed.

References

- Azamathulla HM, Ab Ghani A (2012) Genetic programming to predict river pipeline scour. *Pipeline Syst Eng Pract* 1(3):127–132. [https://doi.org/10.1061/\(ASCE\)PS.1949-1204.0000060](https://doi.org/10.1061/(ASCE)PS.1949-1204.0000060)
- Azamathulla HM, Yusoff MAM, Hasan ZA (2014) Scour below submerged skewed pipeline. *Hydrology* 509:615–620. <https://doi.org/10.1016/j.jhydrol.2013.11.058>
- Azimi H, Shiri H (2020) Ice-seabed interaction analysis in sand using a gene expression programming-based approach. *Appl Ocean Res* 98:102120. <https://doi.org/10.1016/j.apor.2020.102120>
- Azimi H, Bonakdari H, Ebtehaj I, Talesh SHA, Michelson DG, Jamali A (2017) Evolutionary Pareto optimization of an ANFIS network for modeling scour at pile groups in clear water condition. *Fuzzy Sets Syst* 319:50–69
- Azimi H, Bonakdari H, Ebtehaj I (2019a) Design of radial basis function-based support vector regression in predicting the discharge coefficient of a side weir in a trapezoidal channel. *Appl Water Sci* 9(4):78. <https://doi.org/10.1007/s13201-019-0961-5>
- Azimi H, Bonakdari H, Ebtehaj I, Shabanlou S, Talesh SHA, Jamali A (2019b) A pareto design of evolutionary hybrid optimization of ANFIS model in prediction abutment scour depth. *Sādhanā* 44(7):169
- Bonakdari H, Ebtehaj I (2017) Scour depth prediction around bridge piers using neuro-fuzzy and neural network approaches. *Int J Civil Environ Eng* 11(6):835–839. <https://doi.org/10.5281/zenodo.1131934>
- Brørs B (1999) Numerical modeling of flow and scour at pipelines. *Hydraulic Eng* 125(5):511–523. [https://doi.org/10.1061/\(ASCE\)0733-9429\(1999\)125:5\(511\)](https://doi.org/10.1061/(ASCE)0733-9429(1999)125:5(511))
- Chiew YM (1993) Effect of spoilers on wave-induced scour at submarine pipelines. *Waterway Port Coastal Ocean Eng* 119(4):417–428
- Dey S, Singh NP (2008) Clear-water scour below underwater pipelines under steady flow. *Hydraulic Eng* 134(5):588–600. [https://doi.org/10.1061/\(ASCE\)0733-9429\(2008\)134:5\(588\)](https://doi.org/10.1061/(ASCE)0733-9429(2008)134:5(588))
- Eberhart R, Kennedy J (1995) A new optimizer using particle swarm theory. In *Micro Machine and Human Science, Proceedings of the Sixth International Symposium on IEEE*, 39–43. <https://doi.org/10.1109/MHS.1995.494215>
- Etemad-Shahidi A, Yasa R, Kazeminezhad MH (2011) Prediction of wave-induced scour depth under submarine pipelines using machine learning approach. *Appl Ocean Res* 33(1):54–59. <https://doi.org/10.1016/j.apor.2010.11.002>
- Fredsoe J, Hansen EA, Mao Y, Sumer BM (1988) Three-dimensional scour below pipelines. *Offshore Mechan Arctic Eng* 110(4):373–379. <https://doi.org/10.1115/1.3257075>

- Jang JS (1993) ANFIS: adaptive-network-based fuzzy inference system. *IEEE Trans Systems, Man, Cybern* 23(3):665–685. <https://doi.org/10.1109/21.256541>
- Moncada-M AT, Aguirre-Pe J (1999) Scour below pipeline in river crossings. *Hydraulic Eng* 125(9):953–958. [https://doi.org/10.1061/\(ASCE\)0733-9429\(1999\)125:9\(953\)](https://doi.org/10.1061/(ASCE)0733-9429(1999)125:9(953))
- Myrhaug D, Rue H (2003) Scour below pipelines and around vertical piles in random waves. *Coast Eng* 48(4):227–242
- Najafzadeh M, Barani GA, Azamathulla HM (2014a) Prediction of pipeline scour depth in clear-water and live-bed conditions using group method of data handling. *Neural Comput Applic* 24(3–4):629–635. <https://doi.org/10.1007/s00521-012-1258-x>
- Najafzadeh M, Barani GA, Hessami Kermani MR (2014b) Estimation of pipeline scour due to waves by GMDH. *Pipeline Syst Eng Pract* 5(3):06014002. [https://doi.org/10.1061/\(ASCE\)PS.1949-1204.0000171](https://doi.org/10.1061/(ASCE)PS.1949-1204.0000171)
- Shabanlou S, Azimi H, Ebtehaj I, Bonakdari H (2018) Determining the scour dimensions around submerged vanes in a 180 bend with the gene expression programming technique. *J Mar Sci Appl* 17(2): 233–240. <https://doi.org/10.1007/s11804-018-0025-5>
- Sumer M, Fredsoe J (1990) Scour below pipelines in waves. *Waterway Port Coastal Ocean Eng* 116(3):307–323. [https://doi.org/10.1061/\(ASCE\)0733-950X\(1990\)116:3\(307\)](https://doi.org/10.1061/(ASCE)0733-950X(1990)116:3(307))
- Sumer BM, Truelsen C, Sichmann T, Fredsøe J (2001) Onset of scour below pipelines and self-burial. *Coast Eng* 42(4):313–335. [https://doi.org/10.1016/S0378-3839\(00\)00066-1](https://doi.org/10.1016/S0378-3839(00)00066-1)
- Teh TC, Palmer AC, Bolton MD, Damgaard JS (2006) Stability of submarine pipelines on liquefied sea beds. *Waterway Port Coastal Ocean Eng* 132(4):244–251. [https://doi.org/10.1061/\(ASCE\)0733-950X\(2006\)132:4\(244\)](https://doi.org/10.1061/(ASCE)0733-950X(2006)132:4(244))
- Wu Y, Chiew YM (2012) Three-dimensional scour at submarine pipelines. *Hydraulic Eng* 138(9):788–795. [https://doi.org/10.1061/\(ASCE\)HY.1943-7900.0000583](https://doi.org/10.1061/(ASCE)HY.1943-7900.0000583)